

Temperature dependent structural studies on the spin correlated system A_2FeCoO_6 (A= Sm, Eu, Dy and Ho) using synchrotron radiation

Cite as: AIP Advances 7, 055826 (2017); <https://doi.org/10.1063/1.4977497>

Submitted: 24 September 2016 • Accepted: 21 November 2016 • Published Online: 23 February 2017

G. R. Haripriya, R. Pradheesh, M. N. Singh, et al.



View Online



Export Citation



CrossMark

ARTICLES YOU MAY BE INTERESTED IN

The order of magnetic phase transitions in disordered double perovskite oxides Sm_2FeCoO_6 and Dy_2FeCoO_6

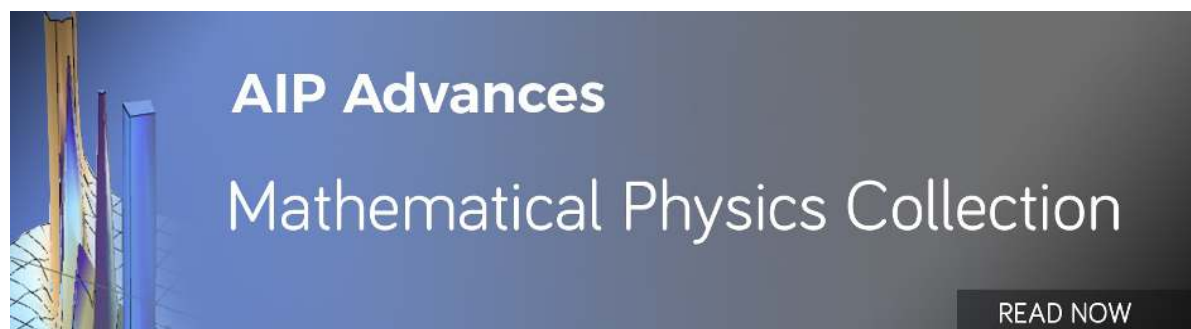
AIP Advances 8, 101340 (2018); <https://doi.org/10.1063/1.5042757>

Dielectric response of the magnetic perovskite oxide Eu_2FeCoO_6

AIP Conference Proceedings 1942, 130052 (2018); <https://doi.org/10.1063/1.5029122>

Magnetization-steps in Y_2CoMnO_6 double perovskite: The role of antisite disorder

Journal of Applied Physics 116, 123907 (2014); <https://doi.org/10.1063/1.4896399>



Temperature dependent structural studies on the spin correlated system A_2FeCoO_6 (A= Sm, Eu, Dy and Ho) using synchrotron radiation

G. R. Haripriya,¹ R. Pradheesh,¹ M. N. Singh,² A. K. Sinha,² K. Sethupathi,¹ and V. Sankaranarayanan¹

¹Department of Physics, IIT Madras, Chennai, Tamil Nadu 600 036, India

²Indus Synchrotron Utilization Division, RRCAT, Indore, Madhya Pradesh 452 013, India

(Presented 2 November 2016; received 24 September 2016; accepted 21 November 2016; published online 23 February 2017)

The temperature dependent structural studies carried out on the spin-correlated system A_2FeCoO_6 (A= Sm, Eu, Dy and Ho) or AFMO (A= Sm, E, D and H), using synchrotron radiation is presented. Owing to the large absorption cross-sections of the rare earths; Eu, Sm and Dy for neutrons, synchrotron radiation is one of the best available candidates for probing the system. The perovskite phase formation is inferred from laboratory XRD with Cu K_α source. The temperature dependent synchrotron X-ray diffraction (SXRD) experiments show the coexistence of monoclinic $P2_1/n$ and orthorhombic $Pbnm$ phases in Ho and Dy, while Eu and Sm are formed in single phase $Pbnm$. The temperature dependent DC magnetization measurements infer the presence of many interesting features such as thermal hysteresis, magnetic irreversibility, spin re-orientation, re-entrant magnetization and negative magnetization. © 2017 Author(s). All article content, except where otherwise noted, is licensed under a Creative Commons Attribution (CC BY) license (<http://creativecommons.org/licenses/by/4.0/>). [<http://dx.doi.org/10.1063/1.4977497>]

I. INTRODUCTION

Magnetic double perovskite (DP) materials of the form $A_2BB'O_6$ (A: an alkaline earth or rare earth cation, B, B': transition metal cation) widely find applications as sensors, refrigerants etc. One of the well-studied double perovskites, Sr_2FeMoO_6 (SFMO) has shown very high magnetoresistance (MR) above room temperature, which turned out to be the motive force for the search for other DP systems.¹ In general, antisite disorder (ASD) - some of the B - site ions occupying the B' - sites and vice versa - plays a key role in the magneto-structural aspects of a DP. The ASD can control the response of the material to the applied stimuli.² When B - site disorder is present in a magnetic material, it can lead to lattice or spin frustrations. This results in the reduction of ferromagnetic moment of the material. The magnetic frustrations in the material can give rise to kinetic arrest of the spins, leading to a spin glass state for the material.³

The tetragonal spin glass system Sr_2FeCoO_6 (SFCO) belongs to the class of B (B') - site disordered perovskite materials. The disordered B - sites with Fe and Co, of SFCO was confirmed with the help of neutron diffraction due to the incapability of X-rays to distinguish between two nearest neighbour occupants of the periodic table.³ Sr_2FeCoO_6 is a promising candidate for spintronic applications as it exhibits a strong exchange bias as well as a negative magnetoresistance of 63% at 14 K in the presence of 12 T magnetic field.⁴ The existence of mixed valence states of both Fe (4+, 3+) and Co (4+, 3+) in the sample causes the unusual physical properties exhibited by it. The presence of Jahn-Teller ion, Co^{3+} in intermediate spin state, leads to the observed MR in SFCO. If the A-site ion is substituted with a trivalent rare earth ion, interesting magnetic and transport properties are expected. For a stoichiometrically perfect B-site ordered trivalent rare earth based system, the B/B' - site occupants should be in either 3+/3+ states or 4+/2+ states (or vice versa). In such a scenario, the magnetic contribution from the rare earth along with Co^{3+} Jahn Teller mion can lead to many exotic

phenomena. Also, the A^{3+} - Fe^{3+} interactions can lead to spin fluctuations in the lattice as seen in the case of orthoferrites.⁵

To understand the structural aspect of such a system, X-ray diffraction has its limitations. The B-site cations Fe and Co have similar charge and comparable ionic radii. The value of scattering factor for X-rays is nearly the same for Fe and Co (For Fe 26.1889 e/atom, for Co 27.2091 e/atom for the energy 39.89 keV, NIST standard), which makes the X-rays incapable of distinguishing them. Also, the large values of neutron absorption cross-sections of the rare earths Eu, Sm and Dy rule out the use of neutron diffraction technique to probe the B-sites. The synchrotron based diffraction techniques are known to be more effective and versatile due to the wavelength selectivity and availability of highly intense beam. This can effectively probe interatomic dimensions. The A-site substitution is achieved with the trivalent ions of the rare earths Ho, Dy, Sm and Eu. Here we present the preliminary analysis carried out on the synchrotron diffraction structural data for the samples. The dependence of structure on the A-site ionic radii (Shannon radii) is also addressed.⁶ The primary results from the dc magnetization measurements are also discussed.

II. EXPERIMENTAL

The polycrystalline samples, A_2FeCoO_6 (A= Sm, Eu, Dy and Ho) or AFCO (A= Sm, E, D and H), were synthesized by the conventional sol-gel Pechini method. The high pure (99.9%, Sigma Aldrich) metal nitrates and rare earth oxides (preheated at 700 °C for 6 h prior to synthesis) in stoichiometric amounts were dissolved in de-ionized (DI) water along with citric acid in 3:1 ratio. The well-stirred solution was subjected to slow evaporation at 80°C till gel got formed. Thereafter, it was subjected to heat treatment at 120°C for a few hours till the sample got dried. The precursor formed was then grinded and subjected to successive heat treatments at 600°C for 6 h and 900°C for 36 h with a cooling down to room temperature after every 12 h of heating. The final sintering was done at 1050°C for 36 h with intermediate grindings after each 12 h.⁷ The perovskite phase formation was confirmed by means of room temperature X-ray diffraction (PANalytical X'Pert Pro) with Rietveld refinement using FullProf software.⁸ The structural investigations of the samples AFCO (A= Sm, E, D and H), at temperatures 30 K, 50 K, 100 K, 250 K, 275 K and 300 K, were carried out using synchrotron radiation in transmission geometry at Angle Dispersive X-ray Diffraction beam line (ADXRD) (BL-12) on Indus-2 synchrotron source (RRCAT, India). The wavelength (0.77 Å) and the sample to detector distance were accurately calibrated using the SXRD pattern of LaB₆ NIST standard in the same diffraction geometry. The magnetization data is presented following the Zero Field Cooled warming (ZFC), Field Cooled Cooling (FCC) and Field Cooled Warming (FCW). In ZFC protocol, the sample was cooled down to 5 K without any field. At 5 K, a field of 100 Oe was applied and magnetization was taken from 5 to 320 K (warming mode). In FCC mode, the sample was first cooled down to 5 K without any field and then warmed back to 320 K with a field of 100 Oe (same as ZFC) and the FCC data was taken during the next cooling from 320 K to 5 K in presence of the magnetic field. The FCW was carried out on warming the system from 5 K to 320 K in presence of 100 Oe just after FCC. Magnetization measurements were carried out by means of a SQUID based commercial Vibrating Sample Magnetometer (SVSM MPMS 3, QD, USA).

III. RESULTS AND DISCUSSIONS

The room temperature XRD with Cu K α confirmed the perovskite phase formation. Owing to the scattering factors for X-rays the B-site ordering in the current scenario could not be identified. The orthorhombic $Pbnm$ space group was revealed from room temperature XRD measurements. SXRD data was collected for the temperature range 30 K to 300 K and refinement of the obtained SXRD data was done with FullProf software. The room temperature XRD was taken as the starting model. All the atomic positions as well as the Debye Waller factors were refined for many cycles with a pseudo Voigt peak function having axial divergence asymmetry. The refinement was performed with an orthorhombic ($Pbnm$), monoclinic ($P2_1/n$) and a mixed phase for all the samples, where $Pbnm$ has disordered B-sites and $P2_1/n$ possess B-site ordering. For Eu_2FeCoO_6 (EFCO) and Sm_2FeCoO_6 (SmFCO) the best fit was obtained with orthorhombic $Pbnm$. While for Ho_2FeCoO_6 (HFCO) and

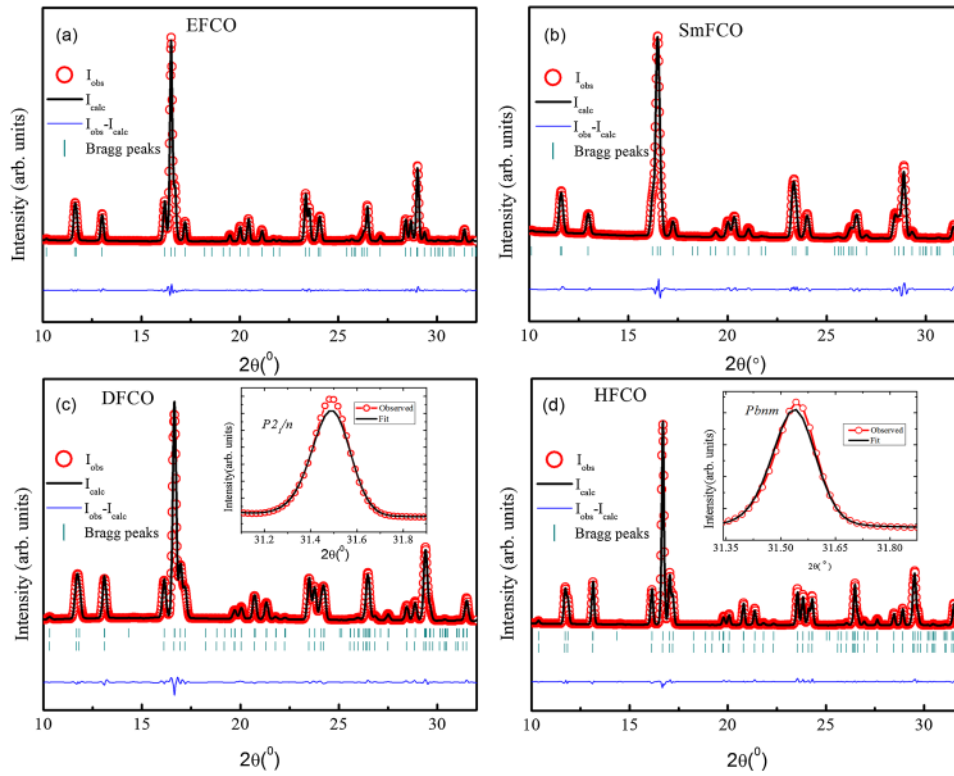


FIG. 1. Room temperature SXRD patterns of (a) $\text{Eu}_2\text{FeCoO}_6$ (EFCO), (b) $\text{Sm}_2\text{FeCoO}_6$ (SmFCO), (c) $\text{Dy}_2\text{FeCoO}_6$ (DFCO) and (d) $\text{Ho}_2\text{FeCoO}_6$ (HFCO). Inset of DFCO shows the misfit at higher angle for single-phase refinement of DFCO using $P2_1/n$ phase and inset of HFCO shows the same for single-phase refinement of HFCO using $Pbnm$ phase.

$\text{Dy}_2\text{FeCoO}_6$ (DFCO), the mixed phase of $P2_1/n$ and $Pbnm$ gave the best fit similar to Y_2CoMnO_6 in which the mixed phase of $Pnma$ and $P2_1/n$ was observed.⁹

Synchrotron diffraction data at room temperature for all the samples are given in Fig. 1 with the Rietveld fitting. The misfits obtained for DFCO with $P2_1/n$ single phase and that for HFCO for $Pbnm$ single phase are shown in the insets of DFCO and HFCO in Fig. 1. The reliability factors and

TABLE I. Reliability factors and lattice parameters for the samples A_2FeCoO_6 (A= Sm, Eu, Dy and Ho) or AFCO (A= Sm, E, D and H), at 300 K after Rietveld refinement.

Compound	HFCO		DFCO		EFCO	SmFCO
Phase 1	$P2_1/n$ (21.59 %)		$P2_1/n$ (29.57 %)		$Pbnm$	$Pbnm$
2	$Pbnm$ (78.41 %)		$Pbnm$ (70.43 %)			
Lattice parameters (Å)	$P2_1/n$	$Pbnm$	$P2_1/n$	$Pbnm$	$Pbnm$	$Pbnm$
a	5.2206(1)	5.2232(1)	5.2426(3)	5.2480(3)	5.3261(2)	5.3515(1)
b	5.5104(1)	5.5139(2)	5.5097(4)	5.5138(2)	5.4974(2)	5.4788(1)
c	7.4912(1)	7.4962(3)	7.5055(5)	7.5157(3)	7.5922(1)	7.6134(2)
	$\beta = 89.979(5)$		$\beta = 90.077(9)$			
χ^2	1.02		1.03		1.33	1.10
R_{Bragg} : Phase 1	2.2		1.82		1.08	1.52
2	2.51		2.13			
R_F : Phase 1	1.9		2.33		1.03	1.10
2	1.35		2.53			
R_{wp}	4.72		5.43		5.25	4.52
R_{exp}	4.66		5.35		4.56	6.72

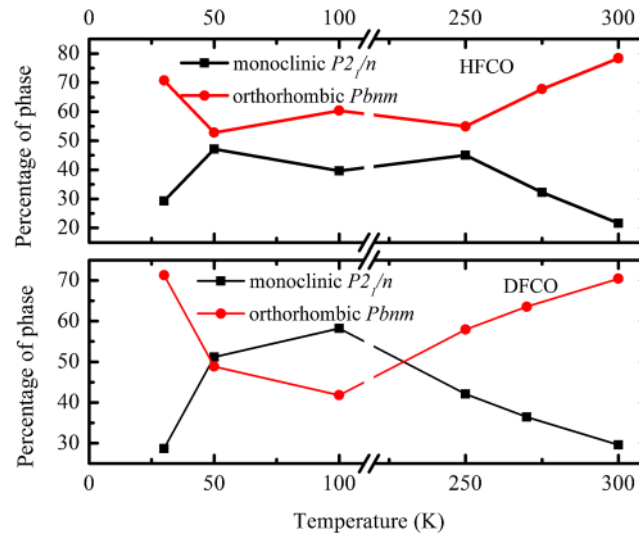


FIG. 2. Temperature dependence of phase fractions of HFCO (top panel) and DFCO (bottom panel) (Solid lines, connecting data points are only guide for eyes). $P2_1/n$ phase is represented with black solid squares and $Pbnm$ phase is represented with red solid circles.

lattice parameters obtained from the refinement for 300 K data for all the samples are tabulated in Table I. The fraction of coexistence of the phases is plotted for HFCO and DFCO in Fig. 2 over the measured temperature range. Here for the monoclinic $P2_1/n$ phase, Fe and Co were assumed to be in two different sites, 2a and 2b. Thermal behaviour of the orthorhombic unit cell volume of all the compounds is given in Fig. 3. All the samples show nonlinear dependence with a very small variation of the unit cell volume. The volume curve traces out similar path for EFCO and SmFCO above 100 K. An increase of unit cell volume is observed with respect to the ionic radius of the A-site occupant as in the case of orthoferrites and orthocobaltites. The rare earth ionic radius (Shannon radius) is considered to have a valence state of 3+ with a cationic coordination of 8 for $Pbnm$.⁴ The Fe and Co cations are likely to be in 3+ valence state. Possibility of the presence of Jahn-Teller (JT) Co^{3+} ion cannot be ruled out as is in the case of $\text{Sr}_2\text{FeCoO}_6$. Fig. 4 shows the variation of the lattice parameters 'a', 'b', and ' $c/\sqrt{2}$ ' of all the samples, for disordered phase, at the temperatures 30 K, 100 K and 300 K with ionic radius of the trivalent A-site rare earth cation. The variation of lattice parameters

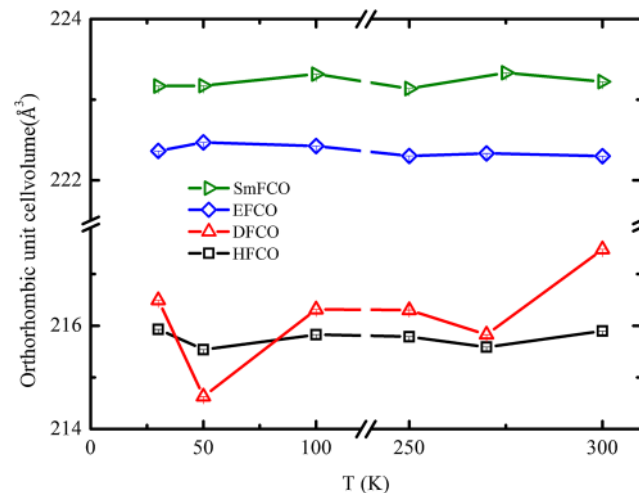


FIG. 3. Temperature dependence of the orthorhombic unit cell volume for the samples: Sm₂FeCoO₆ (SmFCO), Eu₂FeCoO₆ (EFCO), Dy₂FeCoO₆ (DFCO), Ho₂FeCoO₆ (HFCO). (Solid lines, connecting data points are only guide for eyes).

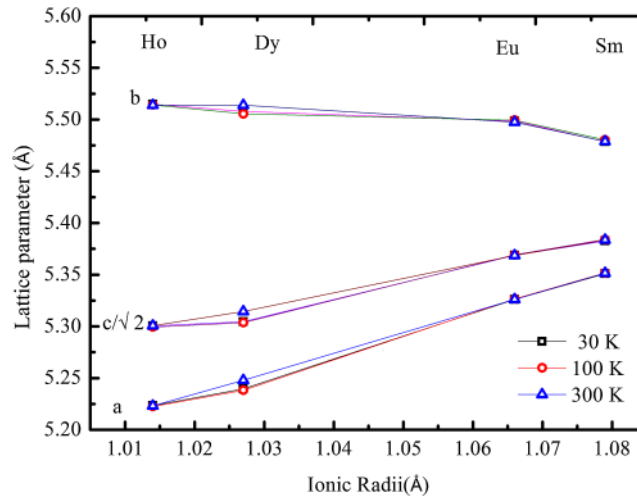


FIG. 4. Variation of lattice parameters (orthorhombic unit cell) of the samples with A-site ionic radii at the temperatures 30 K (black square), 100 K (red circle) and 300 K (blue triangle). (Solid lines, connecting data points are only guide for eyes).

with temperature is observed to be negligibly small for all the samples except DFCO. The parameters 'a' and 'c/√2' increase with the increase in ionic radii while b parameter suffers a decrement as in the case of orthocobaltites (RCoO_3).¹⁰ In orthoferrites (RFeO_3) 'a' and 'c/√2' exhibit a size reduction but 'b' parameter varies irregularly.¹¹ The value of the parameter 'c/√2' lies between b and c, which is a feature of orthorhombic structure. The extensive structural studies carried out by J.-S. Zhou and J. B. Goodenough in RMO_3 (R - rare earths, M - transition metal ions) support the above mentioned observations.¹²

By looking at the variation of B/B'-O bond lengths/bond angles we can surmise the nature of interaction in these systems. For SmFeCO , the $\text{Co/Fe-O}_{\text{ap}}\text{-Co/Fe}$ bond angle shows a linear increase below 100 K while $\text{Co/Fe-O}_{\text{equ}}\text{-Co/Fe}$ decreases linearly below 100 K. Fig. 5 shows the variation of bond angles with temperature. The variation of HFCO bond angles is found to be very small compared to other samples so that a separate plot of the same is shown in Fig. 6. A peculiar behaviour of bond

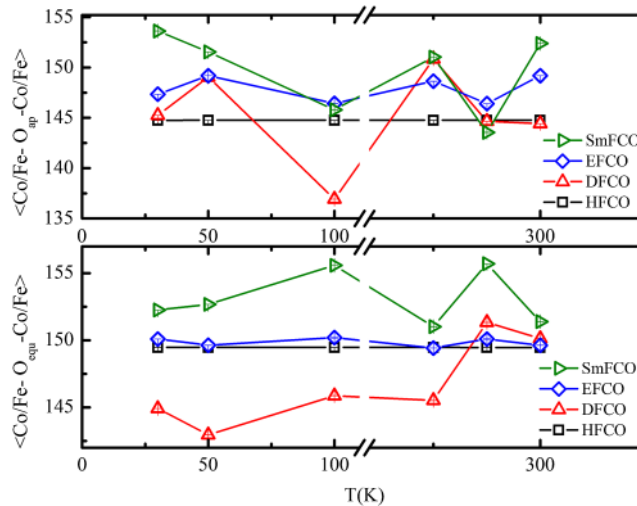


FIG. 5. Temperature dependence of bond angles with apical oxygen (top panel) and equatorial oxygen (bottom panel) for the orthorhombic unit cell for the samples: $\text{Sm}_2\text{FeCoO}_6$ (SmFCO), $\text{Eu}_2\text{FeCoO}_6$ (EFCO), $\text{Dy}_2\text{FeCoO}_6$ (DFCO), $\text{Ho}_2\text{FeCoO}_6$ (HFCO). (Solid lines, connecting data points are only guide for eyes).

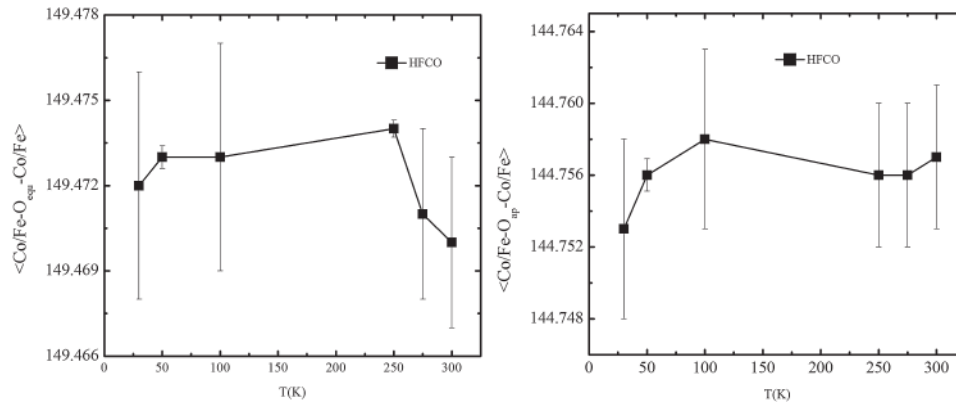


FIG. 6. Temperature variation of bond angles for $\text{Ho}_2\text{FeCoO}_6$ (HFCO). (Solid lines, connecting data points are only guide for eyes).

angles is observed above T_N (≥ 250 K). The bond angle with planar oxygen (equatorial oxygen) follows a similar pattern above 250 K for all the samples except HFCO.

The temperature dependent DC magnetization measurements show unique characteristics for each A-site occupant (Fig. 7). All the three magnetic A-sites give rise to magnetization re-entrance while Eu which has a diamagnetic nature that shows a complete negative magnetization for ZFC up to a temperature of 260 K. Thermal hysteresis and thermomagnetic irreversibility are observed in all the samples. The observed thermal hysteresis for EFCO is lesser compared to the other compositions. The inset of the magnetization curve for EFCO shows the zoomed pattern of FCC and FCW curves

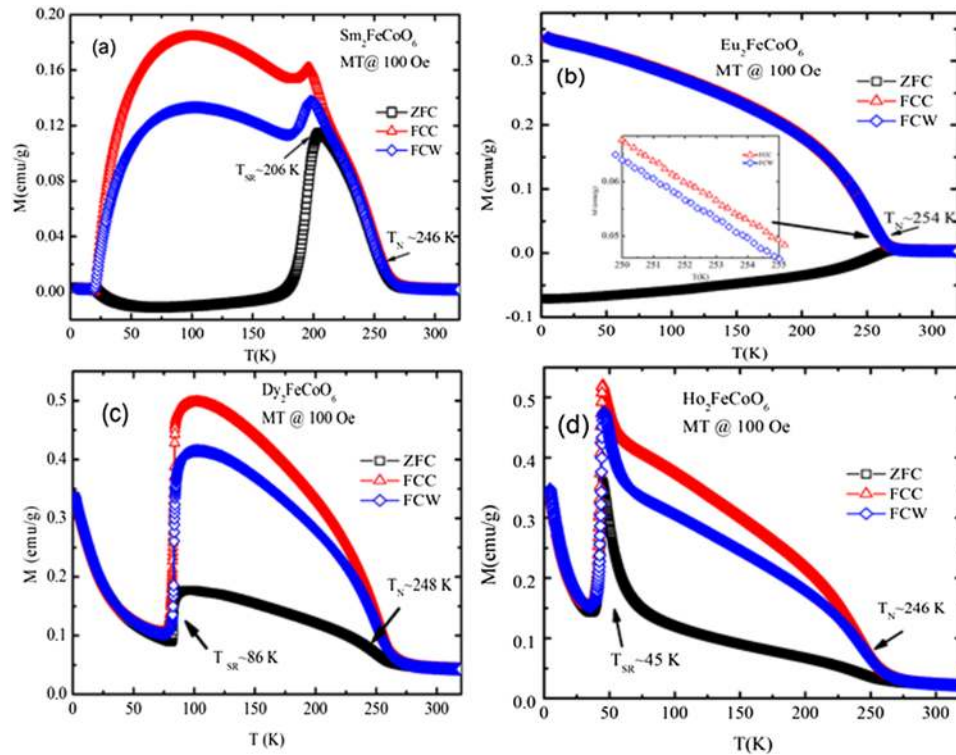


FIG. 7. Temperature dependence of DC magnetization data at 100 Oe for the samples (a) $\text{Sm}_2\text{FeCoO}_6$ (SmFCO), (b) $\text{Eu}_2\text{FeCoO}_6$ (EFCO), inset shows the thermal hysteresis of FCC and FCW between the temperatures 250 K and 255 K, (c) $\text{Dy}_2\text{FeCoO}_6$ (DFCO) and (d) $\text{Ho}_2\text{FeCoO}_6$ (HFCO).

in between 250 K and 255 K. The presence of thermal hysteresis for HFCO and DFCO is due to the presence of mixed structural phases while for an A-site rare earth with higher ionic radii (Eu and Sm) it can be accredited to the presence of a first order phase transition.¹³ The nature of observed irreversibility in FCC and FCW for HFCO and DFCO, suggests that it could be due to mixed magnetic interaction or frustration of the spins. The presence of mixed phases in HFCO and DFCO, points towards the existence of mixed magnetic interactions.

The Neel temperatures (T_N), extracted from the first derivative taken on ZFC curves at 100 Oe for the samples are found to be in the range 246 K – 254 K. On comparing the observed T_N with that of the respective orthoferrites (640 K- 680 K), it can be inferred that the magnetic interactions of Fe and Co lead to the lowering of T_N values obtained for the combined system from that of orthoferrites.⁵ The magnetization data of the samples with magnetic A-site viz., HFCO, DFCO and SmFCO at low temperatures exhibits other features, which can be attributed to the spin re-orientation transition, which is normally observed in rare earth orthoferrites.⁵ The re-orientation of Fe lattice is absent in EFCO as in the case of EuFeO_3 , where a diamagnetic A- site (Eu^{3+}) is present.⁵ The rare earth ordering, which usually occurs at lower temperatures (below 5 K), could not be observed due to instrumental limitations. In the case of SmFCO, the observed spin re-orientation is in the range of 206 K - 180 K which is considerably less than the spin re-orientation temperature (T_{SR}) of SmFeO_3 (480 K - 433 K, 480 K- 450 K).^{5,14} For DFCO the spin reorientation happens through the range 86 K - 81 K, which is higher than that observed for the orthoferrite counter-part. In HFCO, the re-orientation of Fe lattice occurs between the temperatures, 45 K and 37 K, which is less than that observed for HoFeO_3 (65 K – 53 K, 58 K - 51 K).^{5,15} The variation of T_{SR} observed for AFCO, compared to the respective orthoferrites, could be due to the lattice strain induced by the presence of Co ions. Interestingly, it can be noted that the compounds with a magnetic A-site show magnetization re-entrance. The complete explanation of the magnetization data demands further detailed investigations.

IV. CONCLUSIONS

The double perovskite oxides AFCO (A= Sm, Eu, Dy and Ho) were synthesized in polycrystalline form using citrate based sol-gel method. The structural aspects were established via Rietveld refinement of the synchrotron diffraction data for selected temperatures. The presence of mixed structural phases, composed of orthorhombic and monoclinic phases in the samples with lower cationic radii (Ho, Dy) is observed from the Rietveld refinement. However, *Pbnm* is the only phase present in SmFCO and EFCO. The temperature dependent magnetization data reveal unique characteristics for each of these compounds. Thermal hysteresis of the FC curves is observed for all the samples. The Neel temperatures observed for the samples are in the range 246 K – 254 K. The compounds HFCO, DFCO and SmFCO exhibit spin re-orientation transitions as in the case of respective orthoferrites. EFCO shows a negative ZFC magnetization up to 260 K. Further studies are on the way to unveil the cause of crude features observed.

ACKNOWLEDGMENTS

HGR, PR, KS and VSN thank IITM for funding SVSM. HGR acknowledge Mr. P. Seenivasan for his extended help during magnetic measurements.

¹ J. Navarro, C. Frontera, L. I. Balcells, B. Martinez, and J. Fontcuberta, *Phys. Rev. B* **64**, 092411 (2001).

² D. Sanchez, M. Garcia-Hernandez, J. L. Martinez, J. A. Alonso, M. J. Martinez-Lope, M. T. Casais, and A. Møllergaard, *J. Magn. Magn. Mater.* **242**, 729 (2002).

³ R. Pradheesh, H. S. Nair, V. Sankaranarayanan, and K. Sethupathi, *Appl. Phys. Lett.* **101**, 142401 (2012).

⁴ R. Pradheesh, H. S. Nair, C. M. N. Kumar, J. Lamsal, R. Nirmala, P. N. Santhosh, W. B. Yelon, S. K. Malik, V. Sankaranarayanan, and K. Sethupathi, *J. Appl. Phys.* **111**, 053905 (2012).

⁵ Z. Zhou, L. Guo, H. Yang, Q. Liu, and F. Ye, *J. Alloys and Compounds* **583**, 21 (2014).

⁶ R. D. Shannon, *Acta Cryst. A* **32**, 751 (1976).

⁷ I. G. Deac, S. V. Diaz, B. G. Kim, S. W. Cheong, and P. Schiffer, *Phys. Rev. B* **65**(17), 174426 (2002).

⁸ J. Rodriguez-Carvajal, *Physica B* **192**, 55 (1993).

⁹ H. S. Nair, R. Pradheesh, Y. Xiao, D. Cherian, S. Elizabeth, T. Hansen, T. Chatterji, and Th. Bruckel, *J. Appl. Phys.* **116**, 123907 (2014).

- ¹⁰ J. A. Alonso, M. J. Martínez-Lope, C. de la Calle, and V. Pomjakushin, *J. Mater. Chem.* **16**, 1555 (2006).
- ¹¹ A. Berenov, E. Angeles, J. Rossiny, E. Raj, J. Kilner, and A. Atkinson, *Solid State Ionics* **179**, 1090 (2008).
- ¹² J.-S. Zhou and J. B. Goodenough, *Phys. Rev. Lett.* **94**, 065501 (2005).
- ¹³ H. Kuwahara, Y. Tomioka, A. Asamitsu, Y. Moritomo, and Y. Tokura, *Science* **270**, 961 (1995).
- ¹⁴ S. Cao, H. Zhao, B. Kang, J. Zhang, and W. Ren, *Scientific Reports* **4**, 5950 (2014).
- ¹⁵ M. Shao, S. Cao, Y. Wang, S. Yuan, B. Kang, J. Zhang, A. Wu, and J. Xu, *J. Cryst. Growth* **318**, 947 (2011).